Supplementary Appendix

This appendix has been provided by the authors to give readers additional information about the work.

High-Resolution and Non-Invasive Fetal Exome Screening

Supplementary Appendix

Harrison Brand, Ph.D.[1-5,★], Christopher W. Whelan, Ph.D.[11,4,5★], Michael Duyzend, M.D., Ph.D.[1,4,6], John Lemanski, B.Sc.[1], Monica Salani, Ph.D.[1], Stephanie P. Hao, M.Sc.[1,3], Isaac Wong, B.Sc.[1], Elise Valkanas, B.Sc.[1,4,7], Caroline Cusick, M.Sc.[5], Casie Genetti, M.S., C.G.C[8], Lori Dobson, M.S., C.G.C.[9], Courtney Studwell, M.S., C.G.C.[9], Kathleen Gianforcaro, B.A.[9], Louise Wilkins-Haug[10], Stephanie Guseh, M.D.[10], Benjamin Currall, Ph.D.[1], Kathryn Gray, M.D., Ph.D.[1,10], Michael E. Talkowski, Ph.D.[1,2,4,5]

1. Center for Genomic Medicine, Massachusetts General Hospital, Boston, MA
2. Department of Neurology, Massachusetts General Hospital and Harvard Medical School
3. Pediatric Surgical Research Laboratory, Department of Surgery, Massachusetts General Hospital, Boston, MA
4. Program in Medical and Population Genetics, Broad Institute of MIT and Harvard, Cambridge, MA
5. Stanley Center for Psychiatric Research, Broad Institute of MIT and Harvard, Cambridge, MA
6. Department of Pediatrics, Division of Genetics and Genomics, Boston Children's Hospital, Boston, MA
7. Program in Biological and Biomedical Sciences, Division of Medical Science, Harvard Med. School, Boston, MA
8. Manton Center for Orphan Disease Research, Boston Children's Hospital, Boston, MA
9. Center for Fetal Medicine and Reproductive Genetics, Brigham and Women's Hospital, Boston, MA
10. Division of Maternal-Fetal Medicine, Brigham and Women's Hospital and Harvard Medical School, Boston, MA

Correspondence: mtalkowski@mgh.harvard.edu; kgray6@bwh.harvard.edu

Table of Contents

Supplementary Methods

Sample Collection and Library Creation

Samples were collected from the Brigham and Women's Hospital (BWH) LIFECODES longitudinal biorepository[1] and the MAPing pregnancy study biorepository based out of the Center for Fetal Medicine at BWH (Table S1-2). This resource was designed to facilitate research on prenatal screening and diagnosis and understanding of the genetic basis of fetal structural anomalies. We collected samples of any gestation with initial technology development focusing on the third trimester, while the 14 samples referred for clinical genetic testing were amassed primarily from first and second trimester (Tables S3, S12). Women were enrolled at prenatal visits during any time of pregnancy and peripheral blood samples were collected in two Streck collection tubes (Streck, La Vista, NE) providing up to 20 mL of maternal blood. Following sample collection, we separated cell free DNA (cfDNA) from maternal serum using Streck's recommended 'Double Spin Protocol 2'. Precipitated maternal leukocytes were used to extract maternal genomic DNA from all samples. To perform extensive benchmarking of maternal variant discovery, we collected maternal germline DNA (gDNA) for 28 mothers and performed standard exome sequencing (ES) at the Broad Institute Genomics Platform (Table S3).

We extracted DNA from the separated cfDNA portion of the serum with a NextPrep Mag cfDNA Isolation kit (Catalog# NOVA-3825-03). We then determined cfDNA fragment size and concentration via Tapestation (cfDNA tapes, Agilent Technologies) and QuBit (Broad Range DNA, Agilent Technologies), respectively. To convert cfDNA to sequenceable fragments, we used NEBNext® Ultra™ II DNA Library Prep Kit for Illumina® from New England Biolabs (NEB) according to the manufacturer's protocols with the following modifications: 1) NEB adapters and USER enzyme steps were replaced with direct ligation of xGen Stubby unique molecular identifier (UMI) adapters ordered from integrated DNA technologies (IDT); and 2) NEB primers were replaced with xGen dual index primer (IDT). After adapter ligation, PCR was then performed for 12 cycles. Following this initial PCR amplification, libraries were multiplexed into batches of up to

16 (up to 8 ug of total material) and exome capture was performed using the Alpha Broad Exome baits from TWIST Bioscience, targeting 194,202 exonic regions, under the IDT xGen Hybridization Protocol. In brief, multiplexed libraries were combined with Human Cot DNA and xGen blocking oligos and dehydrated prior to resuspension in hybridization buffer and baits. After four hours incubation, bait hybridized libraries were combined with buffer resuspended streptavidin beads and several washes were performed to remove any non-hybridized libraries, followed by 15 rounds of on-bead, post-capture PCR. PCR amplified libraries were purified using SPRI bead clean up, and exome libraries were analyzed with a tapestation (D1000, Agilent Technologies) and QuBit (Broad Range DNA, Agilent Technologies), prior to multiplexing and sequencing on an Illumina NovaSeq. We were able to obtain additional material for benchmarking analyses in a subset of the participants in the study, including fetal cord blood collected at delivery (n = 7), paternal DNA (n = 7), and in an additional four cases DNA was extracted from cultured cells derived from an amniocentesis (Table S3).

Sequence Generation

cfDNA libraries were sequenced at the Broad Institute Genomics Platform in pooled, multiplex sequencing runs on an Illumina Novaseq S4 flowcell. Our multiplexing strategy sought to generate as many unique sequencing reads as possible while keeping the raw sequence duplication rates (without considering UMIs) under 75%. We note that at depth of 200x, assuming a fetal fraction of 25% (the median fetal fraction observed across our samples), each target is expected to have mean coverage of approximately 50 reads of fetal origin. For eight samples (MGB038, MGB039, MGB40, MGB016, MGB043, MGB046, MGB047, and MGB048) sequencing was performed across two S4 flowcells and the raw sequencing reads from the two flowcells were pooled and processed together.

Data Processing Workflow Overview

An overview of the data processing workflows is given in Figure S1. The workflow was divided into three main sections, which are described at a high level in this section and in greater detail in subsequent sections of the Supplementary Appendix. The first stage preprocessed raw sequencing reads, built consensus reads for each UMI found in the sequencing data set, and aligned those consensus reads to the reference genome. See "**Alignment and Preprocessing of cfDNA Sequence Data**" for a more detailed description of the methods and tools used in this step of the pipeline. In the next stage of processing, the somatic variant caller Mutect2 was used to generate candidate variant call sites from the

aligned consensus reads (see section "*Variant Detection in cfDNA with Mutect2*"); a machine-learning based approach was then used to train a classifier for each sample's data set to filter variant sites that are likely to be artifacts (see "*cfDNA Variant Filtering*" section) followed by a Bayesian Mixture Model to simultaneously estimate fetal fraction and assign fetal and maternal genotypes to each variant site ("*cfDNA Genotyping*"). Finally, a set of protocols was developed for annotating, interpreting, and curating variant sites to produce a list of potentially clinically relevant variants for each sample ("*Variant Classification*").

Alignment and Preprocessing of cfDNA Sequence Data

The following pipeline was used to generate high quality GRCh38 aligned CRAM files for variant calling. First, UMIs were extracted from each read using the open source fgbio *ExtractUmisFromBam* (https://github.com/fulcrumgenomics/fgbio) from Fulcrum Genomics. Several subsequent steps were performed using tools from the open source Picard toolkit from the Broad Institute of MIT and Harvard (http://broadinstitute.github.io/picard/), beginning with sorting the data by query name using Picard *SortSam*. Illumina adapters were identified and marked with Picard's *MarkIlluminaAdapters*. Reads were then converted to FASTQ with Picard's *SamToFastq*, aligned to the GRCh38 reference genome with the open source BWA-MEM aligner[2], and merged back into a BAM file with Picard's *MergeBamAlignment*. We then removed a small number of degenerate mapped fragments with mapped fragment length smaller than 19bp with the *PrintReads* tool in the open source GATK[3] framework from the Broad Institute (https://gatk.broadinstitute.org). Reads were then grouped by UMI with the fgbio tool *GroupReadsByUmi*. We created consensus duplex reads with fgbio *CallDuplexConsensusReads* with parameters *--error-rate-pre-umi=45 --error-rate-post-umi=30 --min-input-base-quality=10 --min-reads=0*. Consensus reads were filtered with fgbio *FilterConsensusReads* with parameters *--min-reads 0 0 0 --max-read-error-rate 0.35 --max-base-error-rate 0.3 --min-base-quality 40 --max-no-call-fraction 0.25* and then clipped with fgbio *ClipBam* using parameters *--clipping-mode=Hard --clip-overlapping-reads=true*. Mate information was fixed and the mate CIGAR tags were populated with Picard's *FixMateInformation*. Consensus reads were sorted by coordinate using Picard's SortSam. Finally, base quality scores were recalibrated with the GATK *BaseRecalibrator* and *ApplyBQSR* tools. Collection of alignment metrics such as coverage statistics, as well as variant calling, filtering, and genotyping, were then applied to the covered target intervals in the Twist Broad Custom exome kit (Twist Alliance Clinical Research Exome). A publicly available version of the covered targets data is available at:

Covered gene counts were calculated by intersecting this target interval list with the GRCh38 refSeq database[4] downloaded from the UCSC genome browser (NCBI Annotation Release 110). The steps involved in metrics collection, variant calling, filtering, and genotyping are described in detail in the following sections.

Coverage Analysis

We applied the Picard tool *CollectHsSequencingMetrics* to collect coverage statistics across all exome targets based on aligned consensus reads. In Table S3 we report, for each sample, the mean coverage across all target intervals and the fraction of target bases with at least 50x coverage by cfDNA sequencing reads (of mixed maternal and fetal origin). We also multiplied per-target mean coverage metrics for each sample by that sample's estimated fetal fraction to produce the percentage of exome target intervals with a mean estimated fetal read coverage of at least 8x and 10x, and report both values for each sample in Table S4. Finally, in samples with matched paternal gDNA ES, we report the median and inter-quartile range of the number of reads supporting paternal-only alleles in Table S7, "**Genotyping Performance and Coverage Based on Paternal gDNA ES**". These values can be used to infer the distribution of the depth of coverage of these sites by sequencing reads originating from the fetal genome, half of which are expected to support the paternal allele.

Variant Site Detection in cfDNA

We identified candidate variant sites using the open source software tool Mutect2[5] from the Broad Institute of MIT and Harvard with the parameter *--max-mnp-distance 0* (to split multinucleotide variants into separate records). We set the following parameters to generate annotations used in filtering: *-G StandardAnnotation -G StandardHCAnnotation -A MappingQualityZero -A TandemRepeat -A CountNs*. We generated an additional annotation to use in genotyping (see the section **cfDNA Genotyping**) by modifying GATK to add an *InsertSizeRankSum* annotation to each variant based on the fragment sizes of reads supporting the reference and alternate alleles at each site. To produce this annotation, the distribution of the estimated fragment sizes of reads supporting the reference allele was compared to the distribution of the fragment sizes of reads supporting the alternate allele using a Mann-Whitney U test (implemented by GATK's *RankSumTest*). The value of the annotation is the Z score of the U statistic. Fragment sizes were estimated for each read

determined to be informative at each site by the Mutect2/GATK assembly-based calling engine based on the mapped insert size reported by BWA, as reported in the BAM file for each read pair and were adjusted to account for insertions and deletions reported in the CIGAR and mate CIGAR of the read.

cfDNA Variant Filtering

To remove potential false positive (FP) sites due to sequencing, library preparation, or alignment error, variant site filters were developed that included hard filtering rules and a random forest-based classifier that assigned a score to each variant site that reflected the likelihood that the site was a true positive (TP) variant. The filtering rules were:

1. Any sites in the cfDNA sample were filtered if Mutect2 identified more than one alternate allele with the same start position and at least one of the alternate alleles was an indel.

2. A machine learning classifier (described in detail below) was applied to score variants and filter any variants with a score lower than a cutoff determined by assessing sensitivity to a gold standard set of common variants.

3. Indels that were likely recurrent sequencing errors but still passed our random forest filter were hard filtered based on a list of recurrent artifactual indel calls we observed in our data sets. To construct this list we identified every indel site with an allele count of at least 5 in the subset of cfDNA samples from this study that did not have a matched cord blood or amniocentesis sample and were not among the samples that had been referred for genetic testing. From this resulting list we removed any sites that were present at any allele frequency in the gnomAD v3.1.2[6] database. The remaining sites were used to make a catalog, consisting of 969 indels, which we identified as recurrent artifacts in our data. We applied a filter to remove any indels sites with a position and alternate allele that matched one of the sites in this catalog.

4. Any site that was confidently called by Mutect2 and in phase with a SNV site that did not pass one or more of the filters listed above was also filtered. Mutect2 calls certain sets of sites to be in phase with one another based on the number of reads which span more than one site in the set and support the same combination of alleles. This information is recorded in the phase set ID (PID) annotation for the variant. This filter identified clustered sets of sites that represented mapping errors due to reads that likely originated from other paralogous sequences in the genome that contain multiple paralog specific variants.

In addition to the filters listed above, two filters were applied after genotyping (see section **cfDNA Genotyping**) based on identifying variant sites with unexpectedly low counts of reads supporting the alternate allele.

The classifier described in step 2 above was built using a machine learning tool that trained a random forest classifier based upon the principle of positive-unlabeled learning[7], in which only positive training labels are known with certainty in a training data set. We trained a new instance of this classifier for every sample, using only data from that sample. Reasoning that variant sites that are common in the population are likely to be real, we assigned initial positive labels to sites which are present in gnomAD v3[6] with a maximum sub-population frequency (as given by the *AF_popmax* annotation in the gnomAD data) of at least 0.1. All other sites were initially assigned a negative training label. We then trained a random forest with 800 estimators implemented by the scikit-learn package. After training the classifier we then scored each variant with the predicted probability of the site being a true positive according to the classifier. We then identified a cutoff for this score for PASS filter status using GATK's *FilterVariantTranches* tool, which finds optimal cutoffs that result in a requested estimated sensitivity based on a set of common SNPs and indels supplied as resources with the best practices pipeline. In our pipeline implementation we requested sensitivities of 99.5% to the known SNP sites (using the parameter *--snp-tranche 99.5)* and 95.0% to the known indel resources (*--indel-tranche 95.0)*. The following features, which were chosen based on their independence from variant allele fraction and were either generated by Mutect2 or added based on the genomic context of the site's coordinates, were selected for assessment in the random forest:

- *Indel*: Binary feature indicating whether the variant is a SNP or an indel
- *SOR*: Strand-odds-ratio strand bias test statistic
- *MQ*: Root mean squared mapping quality
- *MQRankSum:* Mapping quality bias rank sum test
- *ReadPosRankSum*: Read position bias rank sum test
- *BaseQRankSum*: Test of base quality score bias for reference and alternate alleles
- *MPOS*: Median distance of site from end of read
- *ECNT*: Number of events in the assembled haplotype containing the variant
- *NCount*: Number of reads in the pileup with an N basecall (created in the formation of duplex consensus reads) at the variant site
- *DP*: Depth at the variant site

8

- *SEGDUP*: Binary features indicating whether the site lies within a segmental duplication

- *LCR*: Binary features indicating whether the site lies within a low complexity region as defined by the LCR-hs38 resource provided by Li et al.[8]

- *SIMPLEREP*: Binary feature indicating whether the site lies within an annotated simple repeat

- *STR*: Binary feature indicating whether GATK/Mutect classifies the site as falling within a short tandem repeat sequence.

It should be noted that the fact that a variant was observed in a repetitive genomic region (as annotated by the SEGDUP, LCR, SIMPLEREP, and STR annotations) was used as a feature for training in the classifier, rather than as a hard filter, with the goal of allowing the classifier to make confident calls in those regions of the genome.

cfDNA Genotyping and Estimation of Fetal Fraction

We developed a machine-learning based model which simultaneously estimates fetal fraction and assigns fetal and maternal genotypes to all variant sites observed in cfDNA sequencing data. Our model consists of a constrained Bayesian Gaussian Mixture Model with five components, with each component representing a different combination of maternal and fetal genotypes for an autosomal variant. The mixtures were defined over two dimensions: the variant allele fraction and the fragment size rank sum statistic, which summarizes the difference between fragments sizes of reads supporting the reference and alternate alleles as described in the section **Variant Detection of cfDNA with Mutect2.** We modeled the fetal fraction of the sample as a latent variable (f) and set the mean of the variant allele fraction distribution for each component based on it as follows: If we let 0/0 represent a homozygous reference genotype, 0/1 represent a heterozygous genotype, and 1/1 represent a homozygous alternate genotype, the components and their means are defined as:

- ("cluster 0": fetal 0/1, maternal 0/0): $f / 2$

- ("cluster 1: fetal 0/0, maternal 0/1"): $(1 - f) / 2$

- ("cluster 2: fetal 0/1, maternal 0/1"): 0.5

- ("cluster 3: fetal 1/1, maternal 0/1"): $f + (1 - f) / 2$

- ("cluster 4: fetal 0/1, maternal 1/1"): $1 - (f / 2)$

Each data dimension was modeled independently, i.e. the covariance matrix for each component was diagonal. Prior to running inference on the model's parameters, we removed a subset of sites that appeared to be outliers, including sites with

non-passing filter status (as set by the filtering procedures described above in *cfDNA Variant Filtering*), sites with cfDNA VAF less than 0.025 or greater than 0.975, and sites with fragment size statistics that were missing, less than -4, or greater than 4. To further clean the data, we removed any sites which did not pass an outlier test for cfDNA VAF and fragment size statistics. The outlier test was implemented by fitting an IsolationForest outlier classifier from the *sklearn.ensemble* package to the data with a contamination parameter of 0.05. We defined the genotyping mixture model in Pyro[9] and fit it to the data for each sample using stochastic variational inference. We used Pyro's AutoDelta guide functions to find the maximum *a posteriori* values for each parameter. To initialize the model, we first produced an initial estimate of the fetal fraction. We did this by identifying the location of the cluster of sites in the VAF distribution representing sites which are maternal homozygous variants and heterozygous in the fetus ("cluster 4"). We initialized the fetal fraction by computing the Gaussian kernel density estimate of all sites with VAF less than 0.975 and identifying the peak in the density with the largest value, corresponding to cluster 4, using the *scipy.signal.argrelextrema* function. To estimate the initialization value for the mean of the fragment size statistic distribution, we found the 500 sites with cfDNA VAF closest to the expected VAF for cluster 4 based on the estimated fetal fraction and used their median fragment size statistic value. Once the fragment size statistic distribution mean for the maternal homozygous variant / fetal heterozygous sites was estimated, we initialized the means of the other fragment size component distributions by multiplying this value times the vector *[-1.0, 0.5, 0.0, -0.5, 1.0]* to match the expected relative contributions of maternal vs fetal reads observed for sites in each cluster.

After fitting model parameters using stochastic variational inference, we re-added all sites that were filtered from the model above to the data set and solved for the optimal cluster assignment parameters for every autosomal site by fully enumerating all latent variables, using Pyro's enumeration strategy for discrete latent variables, with a guide function which fixed the learned model parameters but allowed assignment probabilities to vary. We then estimated the likelihood of each possible fetal genotype by summing the cluster component assignment probabilities: the likelihood that the fetal genotype is 0/0 (ref/ref) at the site was the probability of the site's assignment to cluster 1; the likelihood of a 0/1 (ref/alt) fetal genotype is the sum of the assignment probabilities for clusters 0, 2, and 4; and the likelihood of a 1/1 (alt/alt) fetal genotype is the assignment probability for cluster 3. Sites which appeared to be homozygous alternate in the cfDNA sample (i.e., for which the VAF was greater than 0.975) were automatically assigned a homozygous alternate genotype. Similarly, maternal genotype likelihoods were set as follows: the likelihood of a maternal 0/0 genotype was set to the assignment probability

for cluster 0; the likelihood of a maternal 0/1 genotype was set to the sum of the assignment probabilities for clusters 1, 2, and 3; and the likelihood of a maternal 1/1 genotype was set to the assignment probability for cluster 4.

We applied this model to all autosomal variants in every sample, and to variants on chromosome X in samples in which the fetal sex chromosome ploidy was predicted to be XX. For samples with predicted fetal sex chromosome ploidy of XY, we used the model to genotype variants only within the pseudoautosomal regions (PAR) of chromosome X. For chromosome X variants outside of the PAR in XY samples, we defined three gaussian components for each possible pair of maternal and fetal genotypes (excluding variants homozygous in both mother and fetus). We defined these components based on the parameters learned in training the autosomal model as follows: for the cluster representing maternal heterozygous variants where the fetus carries the variant, the VAF mean was set to $1 / (2 - f)$; for the cluster representing maternal heterozygous variants where the fetus does not carry the variant, the VAF mean was set to $(1 - f) / (2 - f)$; and a third cluster represents variants that are homozygous reference and variant in the fetus (i.e. *de novo* mutations) with VAF mean $f / (2 - f)$. The fragment size means for these clusters were set to the means learned in the autosomal model for clusters 1, 3, and 0, respectively, with a variance equal to the fragment size variance from autosomal cluster 0 times 5 (to account for additional variation observed at these sites). We assigned genotypes to these variants by computing the likelihood that each variant was generated by each of these Gaussian components and assigning the variant to that cluster's genotype set accordingly.

After genotyping, we applied two more filters to the resulting variant calls. First, we filtered out calls where the variant allele fraction was too low to have been generated by the cluster representing variants where the fetus is heterozygous and the mother is homozygous reference, cluster 0. To do this, we conducted a lower-tailed binomial test of the observed number of reads supporting the alternate allele out of the total depth at the site, with a binomial probability of $f / 2$, the expected VAF for that cluster, and filtered out any sites where the p-value of this test was less than 1e-5. Second, we filtered out any indel calls where the alternate allele was supported by three or fewer reads, as we found a high error rate in these variants.

Standard ES from gDNA Variant Calling in Maternal, Paternal, Fetal Cord Blood, and Amniocentesis Samples

The gDNA libraries were prepared from maternal, paternal, fetal cord blood, and amniocentesis samples following standard ES protocols at the Broad Institute Genomics Platform (Cambridge, MA). After Illumina sequencing, reads were

aligned, and variants were called following GATK best practices guidelines[3]. Briefly, following marking and clipping of adapter sequences, pre-processed reads were aligned to the human reference using BWA-MEM[2] with default parameters. Duplicate reads were marked using Picard *MarkDuplicates* and excluded from downstream analysis. Base recalibration was performed using GATK *BaseRecalibrator* and *ApplyBQSR* (using known sites of variation from the GATK Reference Bundle). Germline single-nucleotide variants (SNVs) and indels were called for each sample using GATK *HaplotypeCaller* in GVCF mode followed by joint genotyping across all maternal and fetal DNA derived samples and variant filtration with GATK VQSR. To ensure a high-quality set of genotypes for use in benchmarking, we further applied a stringent set of variant filters previously used in large scale familial sequencing projects[10]. Briefly, variant sites were removed if they overlapped low complexity regions of the genome; variant genotypes were filtered that met any of the following criteria: depth less than 10; allele balance < 0.25 or > 0.75; probability of the allele balance (based on a binomial distribution with mean 0.5) below 1e-9; or fewer than 90 of the reads being informative for genotype. For the amniocentesis sample for study participant MGB043, sequencing was performed at Boston Children's Hospital (Boston, MA) using protocols from GeneDx (Stamford, CT). Sequencing data from this sample was re-aligned to hg38 and then re-processed according to the informatics steps listed above; for this sample alone we limited benchmarking evaluations to the intersection of the exome target regions of the Broad Custom Exome kit used for the rest of the samples and the GeneDx kit.

Benchmarking and Evaluations

Variants were compared to "truth" genotype data derived from ES of gDNA from either matched cord blood, amniocentesis, maternal DNA collected from leukocytes, or paternal samples (see section **gDNA ES Variant Calling in Maternal, Paternal, Fetal Cord, and Amniocentesis Samples**). For the comparison of cfDNA variants to cord blood or amniocentesis, we conducted five sets of evaluations, reported in Table S5,6,8,10:

- A site-level comparison of variants that were not removed by our filtering method (see Supp. Methods section "**cfDNA Variant Filtering**") which did not consider the fetal genotype at the site (Table S10 , "**After Filter Variant Detection**"). This evaluation provides an assessment of the limits to sensitivity of cfDNA sequencing at the depths used in this study, after an attempt to remove sequencing artifacts and other errors from the sequencing data. As with the **Unfiltered Variant Detection** evaluation below, we excluded

maternal variants that were not transmitted to the fetus from this evaluation so that the PPV metrics show the ability of the method to distinguish errors from true biological variation.

- A site-level comparison of all variant sites detected in the cfDNA sequencing data (and therefore of either maternal or fetal origin, or both) without regard to the ultimate filter status or fetal genotype assigned to the site by our bioinformatic pipelines (also in Table S10, "**Unfiltered Variant Detection**"). This evaluation provides an assessment of the theoretical limits to sensitivity of cfDNA sequencing at the depths used in this study without attempting to remove sequencing artifacts and other errors. We excluded any sites which were present in the mother but not transmitted to the fetus (according to the maternal and cord blood or amniocentesis gDNA ES data) and therefore FPs in this evaluation are expected to represent true sequencing or mapping errors, as opposed to failures in fetal/maternal genotyping.

- A comparison of all fetal genotypes assigned by our model to all genotypes called in the cord blood or amniocentesis ES data (Table S5, "**Overall Genotyping Performance**"). This evaluation assesses the accuracy of our genotyping model, which attempts to assign a fetal and maternal genotype to all sites detected in the cfDNA (which is a mixture of cfDNA fragments with maternal and fetal origins). See Supp. Methods section **cfDNA Genotyping** for a description of the genotyping model. In contrast to the "**Unfiltered Variation Detection**" and "**After Filter Variant Detection**" evaluations, untransmitted maternal variants are included. The results of this assessment represent the full ability of our informatic methods to determine the fetal genotype at every site in the exome given only a cfDNA sequencing sample.

- A comparison of all variants that were assigned a fetal heterozygous genotype and a maternal homozygous reference genotype (Table S6, "**Predicted Paternal or *de novo* Variant Detection**") to sites that were present in the cord blood or amniocentesis gDNA ES data but were not present in the maternal gDNA ES data for that participant. In this evaluation, we excluded any variant sites detected in the maternal gDNA ES data from evaluation, and only assessed variants called in the non-invasive fetal sequencing (NIFS) performed exome-wide data which the genotyping pipeline had assigned to the "Fetal 0/1; Maternal 0/0" cluster. This evaluation characterizes the method's accuracy in detecting paternally inherited variants, as well as *de novo* mutations.

- An assessment of the ability of our methods to accurately genotype variants that are heterozygous in the mother (Table S8, "**NIFS Genotype Accuracy for Variants Heterozygous in the Mother**"). This evaluation focuses only on sites where the maternal gDNA ES data indicates that the mother is heterozygous for a variant with passing filter status. These sites are important for recessive disease diagnostics but are more difficult to genotype a low fetal fraction. For this evaluation we report a single accuracy metric which is the percentage of true maternal heterozygous sites that were assigned a passing filter status and the correct fetal genotype by NIFS.

All the above evaluations except for "**NIFS Genotype Accuracy for Variants Heterozygous in the Mother**" were conducted with the *vcfeval* tool from Real Time Genomics[11],[12] (RTG; https://www.realtimegenomics.com/products/rtg-tools), which conducts a haplotype-based analysis to match variants between samples, and is a widely accepted standard for genomic variant calling evaluations. All benchmarking analyses were limited to intervals targeted by the exome capture panel on the autosomes. The "**Unfiltered Variant Detection**" and "**After Filtering Variant Detection**" evaluations in the comparison to cord blood and amniocentesis samples were conducted by matching sites without respect to the called genotype. In these two evaluations the presence of the same variant site, matched on genomic position and alternate allele, in both the cfDNA sample and the confirmation data counted as a true positive (this was achieved using the vcfeval parameter —*squash-ploidy*). The "**Overall Genotyping Performance**" comparison, on the other hand, required each called fetal allele in the output of our pipeline to match the alleles present in the genotypes called in the confirmation data. Benchmarking evaluates true positives (TP), FP, true negatives (TN), and false negatives (FN). Sensitivity and PPV were calculated by RTG *vcfeval* as:

- PPV = TP / (TP + FP)

- Sensitivity = TP / (TP + FN)

For all of the above evaluations except for "**Genotype Accuracy for Variants Heterozygous in the Mother**", we excluded from evaluation all regions where the ES data from the cord blood or amniocentesis samples had coverage of less than 10 reads – in other words, called variant sites in these regions were not counted as TP, FP, or FN. This evaluation was conducted using the same analysis scripts as were used for the "**Genotype Accuracy By Maternal and Fetal Genotype**" reported in Table S9, described below. We note that the metrics presented in this evaluation can be computed by summarizing the results for each of the genotype clusters corresponding to maternal heterozygous variants in Table S9.

In addition to the analyses described above, we also used the matched cord blood or amniocentesis gDNA ES data for a more detailed breakdown of NIFS' sensitivity and genotype accuracy on all confirmed variants in the fetal and maternal exomes (Table S9, "**Genotype Accuracy by Maternal and Fetal Genotype**"). For this evaluation, we compared all NIFS calls made from cfDNA to the union set of all variants called in either the maternal gDNA ES or the cord blood/amniocentesis gDNA ES. For each combination of maternal and fetal genotype present in this comparison set of maternal and fetal variants, we calculated the percentage of sites with matching positions and alternate allele that were present in the raw Mutect2 cfDNA VCF (as reported in Table S10) and the percentage of those sites that were not filtered and were assigned the correct fetal genotype by the cfDNA variant calling pipeline. These evaluations were conducted with a custom analysis script which matched variant calls in the maternal gDNA ES, cord blood or amniocentesis gDNA ES, and cfDNA sequencing data by genomic position and alternate allele (as opposed to the haplotype-based methods implemented in RTG *vcfeval*).

A second set of evaluations compared the maternal genotypes predicted by our model to the variants detected in ES sequencing of maternal gDNA extracted from precipitated maternal leukocytes. The results of this evaluation are reported in Table S11 in two parts, "**Detection of Maternal Variants**" and "**Maternal Genotyping Performance**". We allowed any called variant sites to match for the "**Detection of Maternal Variants**" comparison, regardless of the maternal genotypes assigned by NIFS or gDNA variant calling. We required full genotype matches between gDNA and ES calls for the "**Maternal Genotyping Performance**" evaluation. For these maternal evaluations we excluded any sites for which the maternal gDNA ES data had less than 10x read coverage. These evaluations were conducted using the RTG *vcfeval* tool.

Finally, for participants with matching gDNA ES data derived from a paternal blood sample, we conducted an evaluation of the proportion of sites assigned a non-reference fetal genotype in the cfDNA data, excluding sites that were present in the maternal gDNA ES data, which were present in the paternal gDNA ES data. The results of this evaluation are reported in Table S7, "**Genotyping Performance and Coverage Based on Paternal gDNA ES**". This evaluation is another way of computing the PPV of NIFS calls that are predicted to be either paternally inherited or *de novo* mutations that supplements the "**Predicted Paternal or *De Novo* Variant Detection**" results reported in Table S6. For this analysis, we used RTG *vcfeval* to calculate the PPV of all calls assigned to cluster 0 (the cluster representing fetal heterozygous and maternal homozygous reference variants) against the set of paternal ES variants, and we limited the evaluation to sites that did not match a variant site in the maternal ES data. We excluded any regions where the paternal ES data had read coverage

of less than 10x from this evaluation. We also report the number of reads supporting the alternate allele for each of these confirmed paternal variants detected by NIFS.

As mentioned above, for sample MGB043, the amniocentesis sample was sequenced at Boston Children's Hospital using a different exome capture kit provided by GeneDx, and we therefore limited all evaluations to the set of exome target intervals covered by both the Twist Custom Exome list used for the NIFS samples and the GeneDx exome targets (n = 194,202 intervals).

Familial Relationship Inference

Predicted genetic relationships (between cfDNA, parental, and cord blood and amniocentesis samples) were confirmed with KING[13] after variant calling. In order to confirm suspected familial relationships in our cohort we filtered the cfDNA variants to include only those with a gnomAD allele frequency (AF_popmax) greater than 0.05 and a quality score for fetal genotype inference greater than 10. Processing the resulting predicted genotyping cluster with KING (parameters *–related –degree 2*), verified that the expected relationships had an estimated proportion of the genome identical by descent (KING metric *PropIBD*) of at least 0.4 (with one exception, a paternal-fetal pair with 0.32 propIBD, which we manually confirmed).

Detection of Copy Number Variants (CNVs)

We developed a sliding-window binning approach to investigate significant deviations in copy state using coverage collected from GATK *CollectReadCounts* with GC correction. Copy states were normalized against a subset of the control NIFSs libraries (absent fetal anomaly cases, Table S12) with GATK *CreateReadCountPanelOfNormals* and *DenoiseReadCounts*. We filtered out highly variable capture intervals with median absolute deviations (MAD) greater than 3rd quartile + 1.5*interquartile range (IQR) in the control cfDNA samples. We then computed the median copy ratio for each sample in bins representing sliding windows across the genome of size 3 MB with an offset of 100 kb. A final filtering step was applied, removing 1 MB bins with >10 of control samples classified as outliers based on a per-bin IQR analysis.

Only one validated CNV event was observed in our study cohort, so we were unable to conduct extensive benchmarking or a sensitivity analysis of CNVs. We note that our previous gDNA ES studies, as reported by Fu et al.[10], have demonstrated accurate CNV discovery beyond the resolution of individual genes – down to routine discovery of events that span >2 exons – and have noted the potential for discovery of CNVs at single exon resolution. Detection of these events in

cfDNA will be difficult due to the mixture of maternal and fetal DNA, but more data will allow for the development of improved methods and thorough benchmarking.

Sex Determination

We explored the ability of NIFS to determine fetal sex given the robust coverage of chrY and chrX. We initially focused on chrY for delineation of sex given that any reads on chrY, beyond a few artifacts, should indicate male fetal sex. In fact, the presence of any coverage (from GATK *CollectReadCounts*), on chrY binned interval was highly discriminatory for sex determination (Figure S3), though exact prediction of chrY copy state, as determined by dividing the median coverage across all intervals chrY by the fetal fraction, remained challenging due to the relatively low and variable coverage on chrY compared with the rest of the genome.

Variant Classification

We analyzed each sample for potentially pathogenic variation in the fetus and mother, using genotypes derived from the cfDNA results. We applied *bcftools*[14] *merge* to create a multisample VCF of all samples with cffDNA sequencing. Using ANNOVAR[15] and bcftools, this merged VCF was annotated with genic and functional consequences (RefSeq[4]), allele frequency (gnomAD v2.1.1 and gnomAD v3.0), REVEL[16] scores, ClinVar[17] annotations (updated 2023-04-30), and per gene disease information such as inheritance type (e.g. recessive) from the Online Mendelian Inheritance in Man (OMIM, version 2022-07-08[18]).

We included variants if they had an allele frequency of <5 or were not reported in gnomAD v2.1.1 and gnomAD v3.0[6]. We excluded synonymous variants. We then created a list from each sample for further review, including all ClinVar annotated Pathogenic/Likely Pathogenic variants, all frameshift/stopgain variants, all predicted splice variants with a Splice AI score[19] > 0.95, all non-frameshift variants > 15 amino acids; and all non-synonymous variants with a REVEL score >0.7. With the exception of ClinVar P/LP variants, variants not passing filters were removed. Of this set, variants with <4 alternate reads, and those determined likely_benign or benign/likely_benign in ClinVar were filtered.

We ascertained fetal genotype using the methods described above with the caveat that for a small subset of indels that were phased with a high quality SNV, we use the SNV genotype given the higher SNV genotype accuracy. Variants in disease genes from OMIM were selected for further analysis. We manually reviewed each of the remaining variants using

the Integrated Genomics Viewer (IGV) and removed variants that appeared to be low quality or were present in multiple

NIFS samples (indicating that they were likely technical artifacts). Variants were reviewed for pathogenicity based on ACMG

criteria[20-22] and clinical relevance was assessed. CNVs were assessed following Clingen and ACMG guidelines provided by

Riggs *et al.*[23]. We identified potential carrier variants for the 28 samples with matching maternal germline exome

sequencing data (Table S3), which we further filtered based on their ClinVar pathogenicity. Variants were considered if they

were listed as pathogenic or likely pathogenic in ClinVar with Clinical Significance corresponding to 2 or more gold stars

(i.e. practice guideline, reviewed by expert panel, or criteria provided with multiple submitters and no conflicts). Variants

with genotypes corresponding to maternal carrier status were selected. As before, variants were reviewed for potential

clinical relevance (Table S14). All identified variants were confirmed by maternal germline ES.

Supplementary Figures

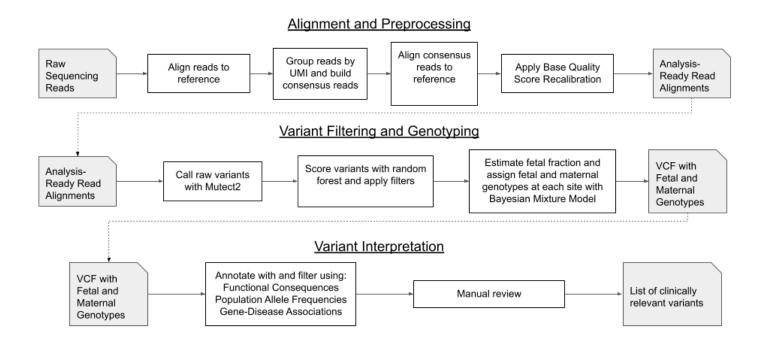**Figure S1.** Bioinformatic Data Processing Flowchart

Figure S1. Data processing is divided into three stages. In the <u>Alignment and Preprocessing</u> stage, raw sequencing reads derived from cfDNA ES are aligned to the reference genome, grouped by UMI, and transformed into a single consensus read for each UMI. Consensus reads are then realigned to the reference and base quality scores are recalibrated,

producing a set of aligned consensus reads that are ready for downstream variant calling and analysis. Next, in the <u>Variant Filtering and Genotyping</u> stage of the workflow, candidate variants sites are identified using Mutect2; variants are filtered using a set of hard filters and a random-forest based model trained on a subset of sites present in that sample; and then a Bayesian Mixture Model is used to simultaneously estimate the fetal fraction and assign fetal and maternal genotypes to each site. Finally, in <u>Variant Interpretation</u> all passing variants are annotated and evaluated to produce a list of clinically relevant variants for interpretation.

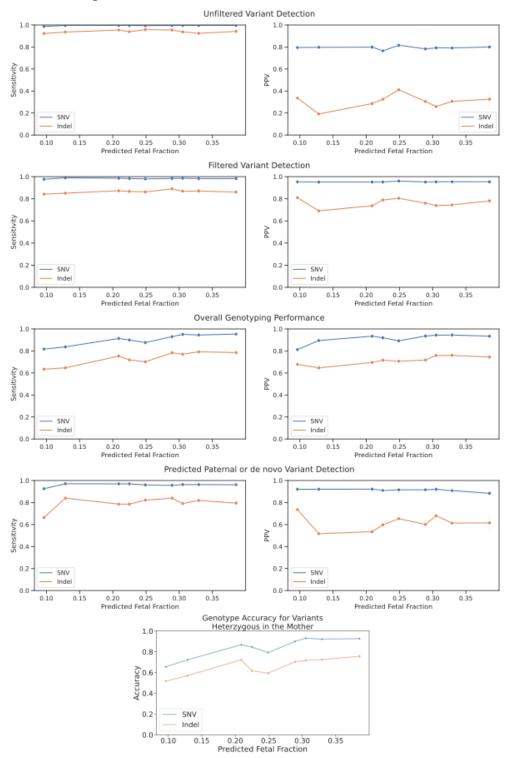## Figure S2. Benchmarking Results

Figure S2. The "Unfiltered Variant Detection", "Filtered Variant Detection", "Overall Genotyping Performance", "Predicted Paternal or *de novo* Variant Detection" and "Genotyping Accuracy for Variants Heterozygous in the Mother" evaluations are plotted against fetal fraction. Theoretical sensitivity and detection of non-maternal variants is strong across fetal fractions, while genotyping accuracy, especially for variants which are heterozygous in the mother, is worse at lower fetal fractions. Sensitivity: TP / (TP + FN); PPV: TP / (TP + FP); Genotype Accuracy: Percent of maternal heterozygous variants assigned the correct fetal genotype.
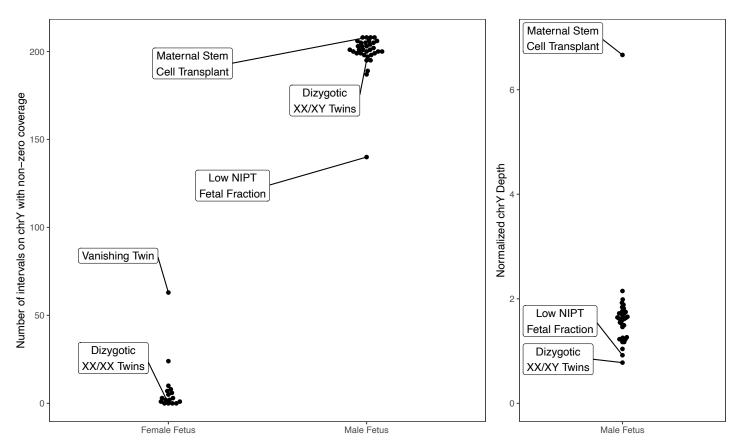
Figure S3. Sex Determination

Figure S3. We were able to separate male and female cases through assessment of sequencing coverage on chrY. Examination of the number of intervals on chrY with mapped sequencing reads allowed us to detect a confirmed male vanishing twin with a female fetus (Table S13), which had read coverage over a much larger proportion of chrY than other samples from pregnancies with female fetuses. Investigating predicted chrY copy state was less accurate, but we did find an extreme case where the mother had received a stem cell transplant from a male donor and therefore had coverage on chrY six times higher than expected. In addition, lower normalized chrY depth distinguished a twin pregnancy with discordant sexes. We also highlight a single sample with lower-than expected fetal fraction, which exhibited depressed coverage on chrY, and a pregnancy with two XX fetuses, which clustered with other samples that had pregnancies with a single XX fetus.

Supplementary Tables

Table S1. Characteristics of Study Samples

Study Characteristics:			
Type of Pregnancy	N	XY	XX
Singleton	49	33	16
Twin: *Monozygotic*	1 pair	0	2
Twin: *Dizygotic*	1 pair	1	1
Fetal Fraction:	Median	IQR	Min-Max
Percentage of fetal cfDNA	25	14-30	6-51
Gestational Age:	1st	2nd	3rd
Trimester	5	9	37
Benchmarking/Confirmation Data:	Parental Germline DNA (Maternal/Paternal)	Cord Blood	Amniocentesis
Germline ES Count	28/7	7	4
NIFS Library Characteristics:	Mean	IQR	Min-Max
Average Per Sample Mean Sequencing Coverage	210	165-232	101-467
Duplication Rate	59	52-63	40-83

IQR - interquartile range

Table S2. Representativeness of Study Participants

CATEGORY	RESPONSE
Disease, problem, or condition under investigation:	cfDNA testing for fetal genetic diseases on maternal plasma in pregnancy.
Special considerations related to:	
Sex and gender	Pregnant individuals who all identified as women.
Age	Reproductive age of women.
Race or ethnic group	Race and ethnicity of this pregnant population is representative of the pregnant population at the recruitment hospital.
Geography	US-based population receiving prenatal care in the Boston area.
Other considerations	The participants had a higher education level and older maternal age than the overall US pregnant population.
Overall representativeness of this trial	Participants are representative of the pregnant population receiving care at the hospital of recruitment.

Table S3. Sample Information

Sample ID	Trimester of Sample	Estimated Fetal Fraction	Fetal Sex	Maternal Germline ES	Paternal Germline ES	Confirmation Sample ES
MGB1	3rd	0.26	XY	No	No	No
MGB2	3rd	0.30	XX	No	No	No
MGB3	3rd	0.27	XY	No	No	No
MGB4	3rd	0.26	XY	No	No	No
MGB5	3rd	0.14	XY	No	No	No
MGB6	3rd	0.25	XY	No	No	No
MGB7	3rd	0.22	XY	No	No	No
MGB8	3rd	0.12	XX	No	No	No
MGB9	3rd	0.18	XY	No	No	No
MGB10	3rd	0.25	XY	No	No	No
MGB11	3rd	0.13	XY	No	No	No
MGB12	3rd	0.30	XX	No	No	No
MGB13	3rd	0.14	XX	No	No	No
MGB14	3rd	0.30	XX	No	No	No
MGB15	3rd	0.20	XX/XY	No	No	No
MGB16	3rd	0.50	XX	No	No	No
MGB17	3rd	0.50	XX	No	No	No
MGB18	3rd	0.25	XY	No	No	No
MGB19	3rd	0.40	XX	No	No	No
MGB20	3rd	0.39	XY	Yes	No	Cord Blood
MGB21	3rd	0.20	XY	No	No	No
MGB22	3rd	0.40	XX	Yes	No	Cord Blood
MGB23	3rd	0.28	XY	No	No	No
MGB24	3rd	0.30	XY	No	No	No
MGB25	3rd	0.36	XY	No	No	No
MGB26	3rd	0.25	XY	Yes	No	Cord Blood
MGB27	3rd	0.24	XX	Yes	No	Cord Blood
MGB28	3rd	0.30	XX	Yes	No	No
MGB29	3rd	0.30	XY	Yes	No	Cord Blood
MGB30	3rd	0.34	XY	Yes	No	No
MGB31	3rd	0.32	XX	Yes	No	Cord Blood
MGB32	3rd	0.28	XX	Yes	No	No
MGB33	3rd	0.30	XY	Yes	No	No
MGB34	2nd	0.13	XY	Yes	No	No
MGB35	2nd	0.14	XX	Yes	No	No
MGB36	1st	0.14	XY	Yes	No	No
MGB37	1st	0.08	XY	Yes	No	No
MGB38	2nd	0.22	XY	Yes	Yes	Amniocentesis
MGB39	1st	0.08	XY	Yes	Yes	No
MGB40	2nd	0.20	XX	Yes	Yes	No
MGB41	2nd	0.09	XY	Yes	Yes	Amniocentesis
MGB42	3rd	0.30	XY	Yes	No	Amniocentesis
MGB43	2nd	0.12	XX/XX	Yes	Yes	Amniocentesis
MGB44	3rd	0.51	XY	Yes	No	No
MGB45	3rd	0.29	XY	Yes	No	Cord Blood
MGB46	1st	0.1	XY	Yes	No	No
MGB47	3rd	0.19	XY	Yes	No	No
MGB48	2nd	0.06	XY	Yes	No	No
MGB49	2nd	0.09	XX	Yes	No	No
MGB50	2nd	0.16	XY	Yes	Yes	No
MGB51	1st	0.14	XY	Yes	Yes	No

Table S4. Sample Coverage and Sequencing Metrics

Sample ID	Mean Coverage	Estimated Duplication Rate	% of Target Bases with at Least 50X Total Coverage	% of Targets with Estimated 8X Mean Fetal Read Coverage	% of Targets with Estimated 10X Mean Fetal Read Coverage
MGB1	135.2	63%	96.32%	97.95%	97.56%
MGB2	110.9	61%	93.87%	97.71%	97.13%
MGB3	143.8	61%	96.39%	97.98%	97.65%
MGB4	101.6	60%	92.20%	97.04%	95.57%
MGB5	119.3	62%	95.06%	92.90%	85.97%
MGB6	168.0	57%	95.59%	97.78%	97.16%
MGB7	174.6	50%	93.30%	95.92%	93.32%
MGB8	173.2	49%	94.19%	86.16%	77.51%
MGB9	202.1	47%	92.47%	92.63%	88.37%
MGB10	192.3	49%	94.52%	97.19%	95.96%
MGB11	159.5	65%	96.27%	93.93%	89.08%
MGB12	221.6	52%	96.61%	98.04%	97.83%
MGB13	215.6	58%	96.64%	95.83%	93.03%
MGB14	139.8	53%	94.33%	97.58%	96.89%
MGB15	307.8	50%	97.29%	97.89%	97.45%
MGB16	214.3	51%	97.04%	98.25%	98.21%
MGB17	228.3	56%	97.14%	98.25%	98.21%
MGB18	202.2	60%	96.97%	98.01%	97.73%
MGB19	184.2	57%	97.00%	98.17%	98.11%
MGB20	160.8	76%	96.81%	98.16%	98.07%
MGB21	344.1	46%	97.03%	97.75%	97.10%
MGB22	268.3	52%	97.15%	98.19%	98.13%
MGB23	128.4	83%	96.16%	97.99%	97.79%
MGB24	173.5	79%	97.39%	98.19%	98.10%
MGB25	465.4	62%	97.48%	98.18%	98.09%
MGB26	104.6	81%	93.84%	96.87%	95.85%
MGB27	209.9	62%	96.59%	97.74%	97.37%
MGB28	265.7	58%	97.24%	98.01%	97.88%
MGB29	320.7	55%	96.64%	96.99%	96.71%
MGB30	188.5	56%	94.83%	97.65%	97.33%
MGB31	229.6	57%	96.73%	97.55%	97.33%
MGB32	229.8	62%	96.87%	97.86%	97.66%
MGB33	198.8	45%	96.84%	98.18%	98.01%
MGB34	157.9	57%	96.59%	95.59%	92.56%
MGB35	167.7	54%	95.89%	95.36%	92.75%
MGB36	131.3	74%	95.89%	95.64%	93.56%
MGB37	204.0	50%	97.08%	89.00%	79.02%
MGB38	277.2	63%	97.36%	97.95%	97.76%
MGB39	220.5	65%	96.30%	91.60%	86.64%
MGB40	202.2	72%	93.81%	92.91%	91.91%
MGB41	215.6	70%	94.14%	87.59%	83.80%
MGB42	210.0	51%	97.22%	98.20%	98.08%
MGB43	330.9	55%	97.62%	97.75%	97.38%
MGB44	102.4	75%	94.42%	98.16%	98.06%
MGB45	201.7	61%	96.55%	97.66%	97.36%
MGB46	293.1	61%	97.32%	96.58%	95.62%
MGB47	247	67%	97.18%	97.90%	97.54%
MGB48	319.6	40%	93.69%	72.38%	64.37%
MGB49	214.5	56%	96.40%	91.73%	87.08%
MGB50	248.5	50%	97.24%	97.47%	96.60%
MGB51	260.1	61%	92.53%	89.38%	87.83%

Table S5. Overall Genotyping Performance

Sample	Mean Target Cov.	Fetal Frac. (%)	Confirmation Method	Overall NIFS Genotyping Performance (%)*									
				Total Variants						SNV		Indel	
				SNV			Indel			Sens.	PPV	Sens.	PPV
				TP	FP	FN	TP	FP	FN				
MGB22	269X	40	Cord ES	20,887	1,446	1,073	324	122	96	95.1	93.5	77.3	72.7
MGB20	161X	39	Cord ES	20,911	1,501	968	354	110	90	95.6	93.3	79.8	76.3
MGB31	232X	32	Cord ES	20,980	1,213	1,219	320	101	85	94.5	94.5	79.2	76.0
MGB29	323X	30	Cord ES	20,654	1,230	1,063	331	105	99	95.1	94.4	77.1	75.9
MGB42	211X	30	Amniocentesis ES	20,072	1,417	1,521	336	131	88	93.0	93.4	79.3	72.0
MGB45	203X	29	Cord ES	20,878	1,389	1,559	331	131	98	93.1	93.8	77.3	71.7
MGB26	104X	25	Cord ES	18,896	2,286	2,662	298	124	128	87.6	89.2	70.2	70.6
MGB27	195X	24	Cord ES	19,040	1,660	2,123	305	121	120	90.0	92.0	71.9	71.6
MGB38	279X	22	Amniocentesis ES	19,289	1,366	1,827	295	129	97	91.4	93.4	75.3	69.6
MGB43	334X	12	Amniocentesis ES	16,451	1,936	3,205	210	115	116	83.7	89.5	64.6	64.6
MGB41	217X	9	Amniocentesis ES	17,670	4,083	3,945	266	126	155	81.8	81.2	63.4	67.9
			Mean:	19,612	1,775	1,924	306	120	107	91.0	91.7	74.1	71.7
			Median:	20,072	1,446	1,559	320	122	98	93.0	93.4	77.1	71.7
			Sum:	215,728	19,527	21,165	3,370	1,315	1,172				

*Evaluates the fetal genotypes assigned to each site by NIFS as compared to the confirmation sample's genotype. All sites in the exome target regions with sufficient depth in the confirmation sample are considered.
Bold indicates values highlighted in letter.

Table S6. Predicted Paternal or *de novo* Variant Detection

Sample	Mean Target Coverage	Fetal Fraction (%)	Confirmation Method	NIFS Predicted Paternal or *de novo* Variant Detection (%)*									
				Total Variants						SNV		Indel	
				SNV			Indel			Sens.	PPV	Sens.	PPV
				TP	FP	FN	TP	FP	FN				
MGB22	269X	40	Cord ES	4,264	585	185	71	58	24	95.8	**87.9**	74.7	55.0
MGB20	161X	39	Cord ES	4,515	568	162	91	43	17	96.5	88.8	84.3	67.9
MGB31	232X	32	Cord ES	4,409	445	171	76	48	17	96.3	90.8	81.9	61.3
MGB29	323X	30	Cord ES	4,411	381	168	83	39	22	96.3	92.1	79.1	68.0
MGB42	211X	30	Amniocentesis ES	4,615	422	196	85	66	17	95.9	91.6	83.3	56.3
MGB45	203X	29	Cord ES	4,684	432	227	99	56	18	95.4	91.6	**84.6**	63.9
MGB26	104X	25	Cord ES	4,385	406	182	83	44	18	96.0	91.5	82.2	65.4
MGB27	195X	24	Cord ES	4,289	426	132	77	52	21	97.0	91.0	78.6	59.7
MGB38	279X	22	Amniocentesis ES	4,306	364	134	77	67	21	97.0	**92.2**	78.6	53.5
MGB43	334X	12	Amniocentesis ES	3,905	335	118	62	58	12	**97.1**	92.1	84.0	51.7
MGB41	217X	9	Amniocentesis ES	4,269	368	343	75	27	38	**92.6**	92.1	**66.4**	73.5
			Mean:	4,368	430	183	80	51	20	96.0	91.1	79.8	61.5
			Median:	4,385	422	171	77	52	18	**96.3**	91.6	**81.9**	61.3
			Sum:	48,052	4,732	2,018	879	558	225				

*Evaluates all sites that NIFS predicts to be heterozygous in the fetus and not present in the mother against sites that are present in the confirmation sample and not present in the maternal gDNA sample.

Excludes regions with coverage of less than 10x in the confirmation sample.

Bold indicates values highlighted in letter.

Table S7. Genotyping Performance and Coverage Based on Paternal gDNA ES

Sample	Mean Target Coverage	Fetal Fraction (%)	Confirmation Method	Non-maternal sites called by NIFS that were present in paternal gDNA ES data				Number of NIFS reads supporting paternal allele at non-maternal sites called by NIFS			
				SNV		Indel		SNV		Indel	
				#	%	#	%	Median	IQR	Median	IQR
MGB38	279X	22	Paternal ES & Maternal ES	4,305	95.6	73	64.6	27	[20-35]	22	[13-31]
MGB40	203X	20	Paternal ES & Maternal ES	3,954	93.4	65	70.7	20	[15-26]	17	[12-23]
MGB50	251X	16	Paternal ES & Maternal ES	4,235	93.8	69	63.9	17	[11-24]	16	[11-22]
MGB43	334X	12	Paternal ES & Maternal ES	3,935	95.0	66	60.6	19	[13-25]	18	[11-22]
MGB41	217X	9	Paternal ES & Maternal ES	4,257	93.8	74	76.3	10	[7-13]	9	[6-12]
MGB51	262X	14	Paternal ES & Maternal ES	4,322	95.5	73	72.3	18	[11-25]	15	[9-20]
MGB39	221X	8	Paternal ES & Maternal ES	3,777	91.1	42	52.5	6	[4-8]	7	[6-9]
			Mean:	4,112	94.0	66.0	65.8	16.7		14.9	
			Median:	4,235	93.8	69	64.6	18		16	
			Sum:	28,785		462					

28

Table S8. Genotyping Accuracy for Maternal Heterozygous Variants

Sample	Mean Target Coverage	Fetal Fraction (%)	Confirmation Method	NIFS Genotyping Accuracy for Variants Heterozygous in the Mother (%)*			
				Total Variants		*Accuracy*	
				SNV	*Indel*	*SNV*	*Indel*
MGB22	269X	40	Cord ES	13,653	261	92.7%	73.6%
MGB20	161X	39	Cord ES	13,644	275	92.8%	**77.8%**
MGB31	232X	32	Cord ES	14,457	273	92.3%	72.5%
MGB29	323X	30	Cord ES	13,234	286	**93.2%**	71.7%
MGB42	211X	30	Amniocentesis ES	12,875	275	89.5%	71.3%
MGB45	203X	29	Cord ES	15,113	304	90.5%	69.7%
MGB26	104X	25	Cord ES	13,283	266	79.3%	59.4%
MGB27	195X	24	Cord ES	13,290	266	84.6%	61.7%
MGB38	279X	22	Amniocentesis ES	12,689	224	86.8%	72.3%
MGB43	334X	12	Amniocentesis ES	13,249	256	72.3%	57.0%
MGB41	217X	9	Amniocentesis ES	13,750	259	**65.6%**	**51.7%**
			Mean:	13,567	268	85.4%	67.2%
			Median:	13,290	266	89.5%	**71.3%**
			Sum:	149,237	2,945		

*Evaluates the accuracy of the fetal genotypes assigned by NIFS for all sites which are heterozygous in the mother (as determined by the maternal gDNA ES).
Bold indicates values highlighted in letter.

Table S9. Genotyping Accuracy by Maternal and Fetal Genotype

Sample	Mean Target Cov.	Fetal Frac. (%)	Fetal and Maternal Genotype	# Sites	Site-level Sens.	Sites Assigned Correct Fetal Genotype (%)	# SNV Sites	SNV Site-level Sens.	SNV Sites Assigned Correct Fetal Genotype (%)	# Indel Sites	Indel Site-level Sens.	Indel Sites Assigned Correct Fetal Genotype (%)
MGB22	269X	40	Fet. 0/1; Mat. 0/0	4,558	99.5	95.4	4,457	99.7	95.9	101	91.1	72.3
			Fet. 0/0; Mat. 0/1	4,448	99.7	89.6	4,361	99.8	90.2	87	94.3	62.1
			Fet. 0/1; Mat. 0/1	7,200	99.9	94.3	7,069	99.9	94.6	131	97.7	80.9
			Fet. 1/1; Mat. 0/1	2,266	100.0	91.2	2,223	100.0	91.5	43	100.0	74.4
			Fet. 0/1; Mat. 1/1	2,122	99.7	90.7	2,081	99.8	91.3	41	95.1	61.0
			Fet. 1/1; Mat. 1/1	5,971	99.9	99.5	5,881	99.9	99.6	90	97.8	92.2
MGB20	161X	39	Fet. 0/1; Mat. 0/0	4,793	99.0	96.2	4,682	99.2	96.5	111	91.9	81.1
			Fet. 0/0; Mat. 0/1	4,839	99.3	90.8	4,738	99.4	91.1	101	94.1	76.2
			Fet. 0/1; Mat. 0/1	6,635	99.8	94.5	6,502	99.9	94.7	133	98.5	82.7
			Fet. 1/1; Mat. 0/1	2,445	99.9	90.4	2,404	99.9	90.9	41	97.6	65.9
			Fet. 0/1; Mat. 1/1	2,326	99.9	95.4	2,277	99.9	95.8	49	100.0	77.6
			Fet. 1/1; Mat. 1/1	5,916	99.8	99.2	5,824	99.8	99.4	92	97.8	89.1
MGB31	232X	32	Fet. 0/1; Mat. 0/0	4,685	99.1	95.9	4,586	99.4	96.3	99	86.9	76.8
			Fet. 0/0; Mat. 0/1	5,012	98.9	94.6	4,900	99.2	95.1	112	84.8	70.5
			Fet. 0/1; Mat. 0/1	7,483	99.8	89.5	7,361	99.8	89.7	122	95.9	73.0
			Fet. 1/1; Mat. 0/1	2,235	99.9	94.1	2,196	99.9	94.4	39	100.0	76.9
			Fet. 0/1; Mat. 1/1	2,383	99.8	97.7	2,347	99.9	97.8	36	94.4	88.9
			Fet. 1/1; Mat. 1/1	5,581	100.0	99.3	5,489	100.0	99.4	92	98.9	91.3
MGB29	324X	30	Fet. 0/1; Mat. 0/0	4,695	99.2	96.0	4,584	99.4	96.5	111	89.2	73.9

			Fet. o/o; Mat. o/1	4,467	99.3	94.5	4,360	99.5	95.1	107	90.7	71.0
			Fet. o/1; Mat. o/1	6,703	99.9	92.3	6,569	99.9	92.7	134	98.5	70.9
			Fet. 1/1; Mat. o/1	2,350	99.7	90.6	2,305	99.8	90.9	45	97.8	75.6
			Fet. o/1; Mat. 1/1	2,263	99.9	97.5	2,232	100.0	97.6	31	96.8	90.3
			Fet. 1/1; Mat. 1/1	5,846	99.9	99.3	5,753	99.9	99.5	93	97.9	89.3
MGB42	211X	30	Fet. o/1; Mat. o/o	4,919	99.3	95.9	4,814	99.5	96.2	105	91.4	81.0
			Fet. o/o; Mat. o/1	4,400	99.1	94.3	4,298	99.3	94.9	102	91.2	68.6
			Fet. o/1; Mat. o/1	6,566	99.8	86.4	6,441	99.8	86.7	125	98.4	71.2
			Fet. 1/1; Mat. o/1	2,184	100.0	86.8	2,136	100.0	87.0	48	100.0	77.1
			Fet. o/1; Mat. 1/1	2,294	100.0	97.6	2,254	100.0	97.9	40	97.5	80.0
			Fet. 1/1; Mat. 1/1	5,703	99.9	99.4	5,614	100.0	99.5	89	97.8	92.1
MGB45	203X	29	Fet. o/1; Mat. o/o	5,042	98.6	95.1	4,921	98.7	95.4	121	93.4	81.8
			Fet. o/o; Mat. o/1	5,584	99.3	94.7	5,455	99.5	95.2	129	90.7	71.3
			Fet. o/1; Mat. o/1	7,434	99.9	86.9	7,312	99.9	87.3	122	98.4	65.6
			Fet. 1/1; Mat. o/1	2,399	99.8	89.4	2,346	99.9	89.7	53	96.2	75.5
			Fet. o/1; Mat. 1/1	2,326	99.8	97.4	2,291	99.9	97.6	35	94.3	82.9
			Fet. 1/1; Mat. 1/1	5,425	99.9	99.4	5,347	99.9	99.5	78	97.4	89.7
MGB26	105X	25	Fet. o/1; Mat. o/o	4,678	98.6	95.6	4,573	98.8	96.0	105	91.4	79.1
			Fet. o/o; Mat. o/1	4,645	99.2	87.8	4,543	99.5	88.2	102	86.3	69.6
			Fet. o/1; Mat. o/1	6,583	99.7	73.3	6,457	99.8	73.7	126	95.2	51.6
			Fet. 1/1; Mat. o/1	2,321	99.9	77.2	2,283	99.9	77.5	38	100.0	57.9
			Fet. o/1; Mat. 1/1	2,387	99.9	96.2	2,342	100.0	96.5	45	95.6	82.2

			Fet. 1/1; Mat. 1/1	5,793	99.8	99.0	5,697	99.8	99.3	96	99.0	86.5
MGB27	195X	24	Fet. o/1; Mat. o/o	4,529	99.0	96.5	4,428	99.2	96.9	101	89.1	77.2
			Fet. o/o; Mat. o/1	4,702	99.5	94.1	4,601	99.7	94.5	101	92.1	76.2
			Fet. o/1; Mat. o/1	6,601	99.7	77.4	6,474	99.8	77.9	127	96.1	55.1
			Fet. 1/1; Mat. o/1	2,253	99.7	83.0	2,215	99.9	83.7	38	92.1	44.7
			Fet. o/1; Mat. 1/1	2,148	99.9	97.0	2,103	100.0	97.3	45	97.8	84.4
			Fet. 1/1; Mat. 1/1	5,870	99.9	99.4	5,774	99.9	99.5	96	99.0	95.8
MGB38	279X	22	Fet. o/1; Mat. o/o	4,543	99.3	96.9	4,444	99.4	97.4	99	95.0	77.8
			Fet. o/o; Mat. o/1	4,401	99.4	95.3	4,310	99.5	95.6	91	97.8	84.6
			Fet. o/1; Mat. o/1	6,307	99.8	79.8	6,206	99.9	80.1	101	98.0	59.4
			Fet. 1/1; Mat. o/1	2,205	100.0	88.5	2,173	100.0	88.7	32	100.0	78.1
			Fet. o/1; Mat. 1/1	2,164	100.0	98.8	2,121	100.0	99.1	43	97.7	83.7
			Fet. 1/1; Mat. 1/1	5,669	100.0	99.6	5,586	100.0	99.7	83	98.8	90.4
MGB43	334X	12	Fet. o/1; Mat. o/o	4,174	99.1	96.7	4,093	99.2	97.0	81	92.6	77.8
			Fet. o/o; Mat. o/1	5,268	99.2	86.4	5,142	99.4	86.8	126	89.7	70.6
			Fet. o/1; Mat. o/1	6,134	99.9	63.2	6,038	99.9	63.5	96	99.0	40.6
			Fet. 1/1; Mat. o/1	2,103	100.0	61.5	2,069	100.0	61.7	34	100.0	52.9
			Fet. o/1; Mat. 1/1	2,090	100.0	98.7	2,060	100.0	98.9	30	100.0	83.3
			Fet. 1/1; Mat. 1/1	5,456	100.0	99.5	5,388	100.0	99.7	68	98.5	85.3
MGB41	217X	9	Fet. o/1; Mat. o/o	4,738	94.3	92.0	4,619	94.7	92.8	119	79.8	62.2
			Fet. o/o; Mat. o/1	5,005	99.2	69.6	4,901	99.5	69.8	104	88.5	59.6
			Fet. o/1; Mat. o/1	6,796	99.8	65.0	6,685	99.9	65.3	111	96.4	47.7

		Fet. 1/1; Mat. 0/1	2,208	99.7	56.7	2,164	99.8	56.9	44	95.5	43.2
		Fet. 0/1; Mat. 1/1	2,493	99.8	91.1	2,442	100.0	91.4	51	98.0	80.4
		Fet. 1/1; Mat. 1/1	5,458	99.9	99.5	5,378	100.0	99.7	80	95.0	87.5

Table S10. Fetal Site Level Variant Detection

Sample	Mean Target Cov.	Fetal Frac. (%)	After Filter NIFS Variant Detection (%)[#]						Unfiltered NIFS Variant Detection (%)[*]					
			SNV			Indel			SNV			Indel		
			Count	Sens.	PPV	Count	Sens.	PPV	Count	Sens.	PPV	Count	Sens.	PPV
MGB22	269X	40	22,996	98.3	95.4	534	85.1	75.8	27,234	99.7	80.6	1,550	93.4	25.8
MGB20	161X	39	22,942	98.1	95.3	538	87.0	80.4	27,508	99.6	79.5	1,099	95.1	39.3
MGB31	232X	32	23,252	98.3	95.4	527	87.0	74.5	28,043	99.7	79.1	1,260	92.4	30.6
MGB29	323X	30	22,761	98.5	95.4	562	86.8	73.9	27,394	99.7	79.2	1,585	93.8	25.9
MGB42	211X	30	22,812	98.6	94.6	556	89.2	74.3	27,582	99.7	78.2	1,489	94.8	27.5
MGB45	203X	29	23,413	98.2	95.8	538	88.6	77.7	28,626	99.5	78.3	1,241	96.1	33.6
MGB26	104X	25	22,428	98.0	96.0	515	86.3	80.5	26,387	99.4	81.6	1,011	95.8	41.1
MGB27	195X	24	22,227	98.3	95.1	522	86.7	78.9	27,633	99.6	76.5	1,257	93.9	32.5
MGB38	279X	22	22,173	98.6	95.2	514	87.3	73.7	26,408	99.7	79.9	1,326	95.4	28.6
MGB43	334X	12	20,647	98.9	95.2	450	85.1	69.1	24,649	99.7	79.7	1,617	93.6	19.1
MGB41	217X	9	22,659	97.7	95.3	503	84.2	81.0	27,112	98.6	79.5	1,186	92.2	33.6
Mean			22,573	98.3	95.3	523	86.7	76.3	27,143	99.5	79.3	1,329	94.2	30.7
Median			22,761	98.3	95.3	527	86.8	75.8	27,394	**99.7**	79.5	1,260	**93.9**	30.6

[#]Evaluates the presence or absence of all sites in the confirmation sample in the filtered list of sites detected by NIFS, without considering genotype. Sites which are maternal only (as determined by the confirmation sample and the maternal gDNA sample), and regions with less than 10x coverage in the confirmation sample, are excluded from the evaluation.
[*]Evaluates the presence or absence of all sites in the confirmation sample in the unfiltered list of sites detected by NIFS, without considering genotype. Sites which are maternal only (as determined by the confirmation sample and the maternal gDNA sample), and regions with less than 10x coverage in the confirmation sample, are excluded from the evaluation.
Bold indicates values highlighted in letter.

Table S11. Maternal Variant Detection and Genotyping Performance against Germline Maternal ES

| Sample | Trimester | Mean Target Cov. | Fetal Frac. | Detection of Maternal Variants | | | | | | | Maternal Genotyping Performance* | | | |
| | | | | Variant Count | | | SNV (%) | | Indel (%) | | SNV (%) | | Indel (%) | |
				TP	FP	FN	Sens.	PPV	Sens.	PPV	Sens.	PPV	Sens.	PPV
MGB20	3rd	160.8	39	21,229	905	724	97.2	96.4	86.2	84.7	96.7	95.9	84.6	83.1
MGB22	3rd	268.7	40	20,883	908	850	97	96.7	82	84	96.1	95.8	79.6	81.2
MGB26	3rd	104.9	25	20,996	790	506	98.1	96.8	85.3	84.3	97.7	96.4	84.1	83.1
MGB27	3rd	195.4	24	20,964	817	368	98.5	96.4	87.9	82.8	98.3	96.3	86.9	81.9
MGB28	3rd	267.9	30	20,506	2,081	1,426	98	95.1	83.8	81.9	93.5	90.8	79.8	77.9
MGB29	3rd	323.6	30	20,938	850	425	98.4	96.4	84	84.2	98	96.1	83.7	84
MGB30	3rd	190	34	20,644	1,086	777	97.3	95.9	82.1	84.4	96.4	95	80.1	82.4
MGB31	3rd	231.6	32	22,006	861	578	97.8	96.6	85.8	86	97.4	96.2	84.2	84.4
MGB32	3rd	231.5	28	20,024	2,504	1,418	98.4	93.6	85.7	78.8	93.4	88.9	78.6	72.3
MGB33	3rd	200.4	30	20,936	824	364	98.5	96.4	86.9	82.3	98.3	96.2	85.4	81
MGB42	3rd	211.4	30	20,497	888	363	98.5	96.1	85.4	81.9	98.3	95.9	84.9	81.5
MGB44*	3rd	102.8	51	12,461	9,028	8,783	78.6	77.7	72.8	70.3	58.7	58	52.7	51
MGB45	3rd	203.3	29	22,490	828	469	98.2	96.7	85.1	82.1	98	96.5	83.9	81
MGB47	3rd	248.3	19	22,824	955	376	98.5	96.1	90.3	80.4	98.4	96	90.1	80.2
MGB34	2nd	158.8	13	21,760	939	259	98.9	95.9	88.8	85.5	98.8	95.9	88.6	85.3
MGB35	2nd	169.1	14	21,775	963	280	98.8	95.8	89.2	79.9	98.7	95.8	88.3	79.1
MGB38	2nd	279.2	22	20,240	977	288	98.7	95.5	90	83.2	98.6	95.4	88.9	82.2
MGB40	2nd	203.3	20	21,060	880	416	98.2	96.1	86.7	79.6	98.1	96	85.5	78.4
MGB41	2nd	216.8	9	21,390	955	311	98.8	95.9	89.4	81.1	98.6	95.7	89.1	80.8
MGB43	2nd	333.6	12	21,051	1,008	287	98.8	95.5	86.1	78.8	98.7	95.4	85.1	77.9
MGB48	2nd	174.2	6	21,026	724	535	97.6	96.7	83.5	85.9	97.5	96.7	82.4	84.7
MGB49	2nd	216	9	21,825	1,065	276	98.9	95.5	88.1	80.3	98.8	95.4	87.4	79.7
MGB50	2nd	250.7	16	20,949	900	357	98.5	96	87.6	81.6	98.3	95.9	87.1	81.1
MGB36	1st	131.9	14	21,184	810	260	98.9	96.4	88.9	87.4	98.8	96.3	87.9	86.3
MGB37	1st	205.8	8	20,933	924	306	98.7	95.9	87.8	79.3	98.6	95.8	87.6	79.1
MGB39	1st	221.9	8	20,956	955	238	99	95.8	87.4	78	98.9	95.6	87.4	78
MGB46	1st	295.3	10	20,716	919	352	98.5	95.9	91.1	81.5	98.3	95.8	90.6	81.1
MGB51	1st	262.2	14	20,576	968	499	98	95.8	85.4	77.3	97.6	95.5	84.9	76.9
			Mean	20,816	1,297	789	97.6	95.4	86.2	81.7	96.3	94.1	84.3	79.8
			Median	20,960	922	372	98.5	96.0	86.5	81.9	**98.3**	95.8	85.2	81.0
			Sum	582,839	36,312	22,091								

* Maternal accuracy dramatically decreases when fetal fraction approaches 50% since the maternal and fetal unique are equivalent allele fractions. Genotype accuracy is calculated by comparing the maternal genotypes assigned by NIFS at each site to genotyping from the gDNA ES of the mother.

Table S12. Clinical Information for Samples

Sample ID	Fetal Sex	Fetal Anomaly	Genetic Testing beyond cfDNA Aneuploidy Screen	Clinical Findings
MGB26*	XY	Bilateral hydronephrosis	No	NA
MGB38	XY	Cleft lip/palate, eye anomalies, possible brain anomaly	Microarray (detected 7q deletion)	Terminal Deletion on chr7
MGB39	XY	Normal ultrasound, both parents carriers of cystic fibrosis	Targeted molecular testing for parental CF variants	Homozygous for pathogenic *CFTR* variant
MGB40	XX	Normal ultrasound, both parents carriers of cystic fibrosis	Targeted molecular testing for parental CF variants	Heterozygous carrier for pathogenic *CFTR* mutation
MGB41	XY	Horseshoe kidney, single umbilical artery	Microarray (normal) and sgNIPT (Vistara) (low risk)	None
MGB42	XY	Heterotaxy, cardiac anomalies	Microarray (normal)	VUS in *ZIC3*
MGB43	XX/XX	Monochorionic-diamniotic twins; twin A: renal anomaly;twin B: congenital diaphragmatic hernia, growth restriction	Microarray (normal x2); research exome sent on twin B	None
MGB44	XY	Omphalocele, ectopia cordis, pulmonary stenosis, hydrops	Microarray (normal); exome sequencing (negative)	None
MGB45	XY	Suspected aortic coarctation	Microarray (normal)	None
MGB46	XY	Increased nuchal translucency	sgNIPT (Vistara) (low risk); declined CVS as NT normalized in the 1st trimester	None
MGB47	XY	Micrognathia	Microarray (normal); Stickler syndrome panel molecular testing, positive for *COL2A1* pathogenic variant	Splicing variant in *COL2A1*
MGB48	XY	Cerebral ventriculomegaly	Microarray (normal) and sgNIPT (Vistara) (low risk)	None
MGB49	XX	Positive aneuploidy screen	Microarray (normal on ongoing pregnancy)	Vanishing Twin
MGB50	XY	Cerebral ventriculomegaly	Microarray (normal) and sgNIPT (Vistara) (low risk)	None
MGB51	XY	Increased nuchal translucency	Microarray (normal) and sgNIPT (Vistara) (low risk)	None

*Excluded from clinical assessment because the patient never received follow up testing

Table S13. Clinically Relevant Variants

	Diagnostic Variants (n = 4)				Other Variants of Interest (n = 3)		
Chr	chr7	chr7	chr12	chrY[#]	chrX	chr7	chr13
Position (hg38)	117559590	155368937-159327017[&]	47982610	1-57227415	137568993	117559590	32340300
Protein Change	p.F508del	-	c.2194-1G>A	-	p.P387_K395del	p.F508del	p.S1982Rfs22
Gene(s)	*CFTR*	-	*COL2A1*	-	*ZIC3*	*CFTR*	*BRCA2*
Disease Description	Cystic Fibrosis	Terminal 4 MB Deletion	Stickler Syndrome	Abnormal Aneuploidy Test	Heterotaxy	Cystic Fibrosis (CF)	Susceptibility to Cancer
Inheritance Mode of Disease	AR	AD	AD	-	XLR	AR	AD
Fetal Genotype	1/1	0/1	0/1	-	0/1	0/1	0/1
Maternal Genotype	0/1	0/0	0/0	-	0/1	0/1	0/0
Paternal Genotype*	0/1	0/0	unknown	-	unknown	0/1	0/1
Clinical Interpretation	High risk for CF	Fetus Affected	Fetus Affected	Result caused by vanishing male twin	VUS in Male Fetus	Maternal, Paternal, & Fetal Carrier	Increased Risk for Cancer
Clinically Validated	Yes	Yes	Yes	Yes	Yes	Yes	No
ID	MGB39	MGB38	MGB47	MGB49	MGB42	MGB40	MGB50
Fetal Sex	XY	XY	XY	XX	XY	XX	XY

*Paternal genotypes derived from separately collected DNA that underwent exome sequencing; see Table S1

[#]Confirmation of a vanishing twin was detected by NIFS during sex inference; see Figure S3

[&]Note that these breakpoints are the minimal breakpoints as defined by identified deleted exons

Table S14. Maternal Carrier Variants

Chr	Position (hg38)	Protein Change	Gene	Disease Description
chr1	150553749	p.Q256Pfs*38	ADAMTSL4	Ectopia Lentis et Pupillae
chr1	169549811	p.R534Q	F5	Factor V Deficiency
chr1	216247094	p.E767Sfs*21	USH2A	Usher Syndrome Type IIA
chr2	44312653	p.M467T	SLC3A1	Cystinuria
chr3	50345495	p.S29P	ZMYND10	Primary Ciliary Dyskinesia
chr4	67740682	p.R262Q	GNRHR	Hypogonadotropic hypogonadism 7 without anosmia
chr4	121854790	p.T211I	BBS7	Bardet-Biedl syndrome
chr4	122927721	p.R83Q	SPATA5	Neurodevelopmental disorder with hearing loss, seizures, and brain abnormalities
chr5	148086434	p.D106Wfs*7	SPINK5	Netherton syndrome
chr7	74783529	p.W193X	NCF1	Chronic granulomatous disease 1
chr7	117559590	p.F508del	CFTR	Cystic Fibrosis
chr7	117559590	p.F508del	CFTR	Cystic Fibrosis
chr7	117559590	p.F508del	CFTR	Cystic Fibrosis
chr7	117559590	p.F508del	CFTR	Cystic Fibrosis
chr8	31141504	p.W1014X	WRN	Werner Syndrome
chr8	142912806	c.1200+1G>A	CYP11B2	Corticosterone Methyloxidase Type I Deficiency
chr10	13112464	p.D128Rfs22	OPTN	Glaucoma
chr11	5227002	p.E7V	HBB	Beta Thalassemia
chr11	59845374	c.79+1G>A	CBLIF	Intrinsic Factor Deficiency
chr11	71491856	p.A573T	NADSYN1	Vertebral, cardiac, renal, and limb defects syndrome 3
chr12	6034812	p.R854Q	VWF	von Willebrand disease
chr12	57244322	p.W98S	STAC3	Congenital myopathy 13
chr12	102866632	p.R158Q	PAH	Phenylketonuria
chr12	110619957	c.173+1G>A	TCTN1	Joubert syndrome 13
chr13	20189413	p.Q57X	GJB2	Deafness
chr13	20189481	p.M34T	GJB2	Deafness, autosomal recessive 1A
chr13	20189546	p.G12Vfs2	GJB2	Deafness
chr13	51944145	p.H862Q	ATP7B	Wilson disease
chr13	51950132	p.G707R	ATP7B	Wilson Disease
chr15	71813573	p.R311Q	NR2E3	Enhanced S-cone syndrome
chr15	89321792	p.G848S	POLG	Mitochondrial DNA Depletion Syndrome
chr16	3243310	p.V726A	MEFV	Familial Mediterranean Fever
chr17	18154189	p.Q2716R	MYO15A	Deafness, autosomal recessive 3
chr17	50167653	p.R77C	SGCA	Muscular dystrophy, limb-girdle, autosomal recessive 3
chr17	80214757	p.G122R	SGSH	Mucopolysaccharidosis type IIIA
chr19	12896249	p.R227P	GCDH	Glutaric Acidemia I
chr19	38502902	p.Q2620X	RYR1	Central Core Disease

Note that 16/28 (57.1%) samples had at least one maternal carrier variant.

References

1. McElrath TF, Lim K-H, Pare E, et al. Longitudinal evaluation of predictive value for preeclampsia of circulating angiogenic factors through pregnancy. Am J Obstet Gynecol 2012;207(5):407.e1-7.

2. Li H. Aligning sequence reads, clone sequences and assembly contigs with BWA-MEM [Internet]. arXiv [q-bio.GN]. 2013;Available from: http://arxiv.org/abs/1303.3997

3. Poplin R, Ruano-Rubio V, DePristo MA, et al. Scaling accurate genetic variant discovery to tens of thousands of samples [Internet]. bioRxiv. 2018 [cited 2019 Nov 21];201178. Available from: https://www.biorxiv.org/content/10.1101/201178v3.abstract

4. O'Leary NA, Wright MW, Brister JR, et al. Reference sequence (RefSeq) database at NCBI: current status, taxonomic expansion, and functional annotation. Nucleic Acids Res 2016;44(D1):D733-45.

5. Benjamin D, Sato T, Cibulskis K, Getz G, Stewart C, Lichtenstein L. Calling Somatic SNVs and Indels with Mutect2 [Internet]. bioRxiv. 2019 [cited 2022 Apr 12];861054. Available from: https://www.biorxiv.org/content/10.1101/861054v1

6. Karczewski KJ, Francioli LC, Tiao G, et al. The mutational constraint spectrum quantified from variation in 141,456 humans. Nature 2020;581(7809):434–43.

7. Bekker J, Davis J. Learning from positive and unlabeled data: a survey. Mach Learn 2020;109(4):719–60.

8. Li H. Toward better understanding of artifacts in variant calling from high-coverage samples. Bioinformatics 2014;30(20):2843–51.

9. Bingham E, Chen JP, Jankowiak M, et al. Pyro: Deep Universal Probabilistic Programming. J Mach Learn Res 2019;20(28):1–6.

10. Fu JM, Satterstrom FK, Peng M, et al. Rare coding variation provides insight into the genetic architecture and phenotypic context of autism. Nat Genet 2022;54(9):1320–31.

11. Cleary JG, Braithwaite R, Gaastra K, et al. Joint variant and de novo mutation identification on pedigrees from high-throughput sequencing data. J Comput Biol 2014;21(6):405–19.

12. Cleary JG, Braithwaite R, Gaastra K, et al. Comparing Variant Call Files for Performance Benchmarking of Next-Generation Sequencing Variant Calling Pipelines [Internet]. bioRxiv. 2015 [cited 2023 Jun 15];023754. Available from: https://www.biorxiv.org/content/10.1101/023754v2

13. Manichaikul A, Mychaleckyj JC, Rich SS, Daly K, Sale M, Chen W-M. Robust relationship inference in genome-wide association studies. Bioinformatics 2010;26(22):2867–73.

14. Danecek P, Bonfield JK, Liddle J, et al. Twelve years of SAMtools and BCFtools. Gigascience [Internet] 2021;10(2). Available from: http://dx.doi.org/10.1093/gigascience/giab008

15. Wang K, Li M, Hakonarson H. ANNOVAR: functional annotation of genetic variants from high-throughput sequencing data. Nucleic Acids Res 2010;38(16):e164.

16. Ioannidis NM, Rothstein JH, Pejaver V, et al. REVEL: An Ensemble Method for Predicting the Pathogenicity of Rare Missense Variants. Am J Hum Genet 2016;99(4):877–85.

17. Landrum MJ, Lee JM, Benson M, et al. ClinVar: improving access to variant interpretations and supporting evidence. Nucleic Acids Res 2018;46(D1):D1062–7.

18. Amberger JS, Bocchini CA, Schiettecatte F, Scott AF, Hamosh A. Omim.org: Online Mendelian Inheritance in Man (OMIM®), an online catalog of human genes and genetic disorders. Nucleic Acids Res 2015;43(Database issue):D789-98.

19. Jaganathan K, Kyriazopoulou Panagiotopoulou S, McRae JF, et al. Predicting Splicing from Primary Sequence with Deep Learning. Cell 2019;176(3):535-548.e24.

20. Gregg AR, Aarabi M, Klugman S, et al. Screening for autosomal recessive and X-linked conditions during pregnancy and preconception: a practice resource of the American College of Medical Genetics and Genomics (ACMG). Genet Med 2021;23(10):1793–806.

21. Harrison SM, Biesecker LG, Rehm HL. Overview of Specifications to the ACMG/AMP Variant Interpretation Guidelines. Curr Protoc Hum Genet 2019;103(1):e93.

22. Richards S, Aziz N, Bale S, et al. Standards and guidelines for the interpretation of sequence variants: a joint consensus recommendation of the American College of Medical Genetics and Genomics and the Association for Molecular Pathology. Genet Med 2015;17(5):405–24.

23. Riggs ER, Andersen EF, Cherry AM, et al. Technical standards for the interpretation and reporting of constitutional copy-number variants: a joint consensus recommendation of the American College of Medical Genetics and Genomics (ACMG) and the Clinical Genome Resource (ClinGen). Genet Med 2020;22(2):245–57.